

Precessional motion of a vortex in a finite-temperature Bose-Einstein condensate

Tomoya Isoshima,* Jukka Huhtamäki, and Martti M. Salomaa
*Materials Physics Laboratory, Helsinki University of Technology,
 P. O. Box 2200 (Technical Physics), FIN-02015 HUT, Finland*
 (Dated: October 25, 2019)

We study the precessing motion of a vortex in a Bose-Einstein condensate of atomic gases. In addition to the former zero-temperature studies, finite temperature systems are treated within the Popov and semiclassical approximations. Precessing vortices are discussed utilizing the rotating frame of reference. The relationship between the sign of the lowest excitation energy and the direction of precession is discussed in detail.

PACS numbers: 03.75.Lm, 03.75.Kk, 67.40.Vs

I. INTRODUCTION

The Gross-Pitaevskii (GP) approximation is often used to analyze the Bose-Einstein condensates (BEC) of atomic gases [1]. The GP approximation only treats the condensate fraction, leaving out the normal component. Therefore, the GP equation treats systems at zero temperature. The Bogoliubov equations [1] describe the excitations supported by the condensate in the zero-temperature limit. The Bogoliubov excitation spectra agree with experimental results, such as the collective oscillation modes (including the Tkachenko waves) [2, 3] of a vortex lattice and those on Bragg spectroscopy [4] of elongated condensates. Since the physical systems exist at finite temperatures, attempts to incorporate effects of temperature into the various approximations have been made [5, 6]. Among these, the Hartree-Fock-Bogoliubov-Popov (Popov) approximation (Sec. V. F in Ref. [7]) is one of the most common finite-temperature approximations.

The Popov approximation treats the density of the normal gas component as a mean field. The condensate is described with the GP equation, extended to include the mean field potential. The excitation spectra and the wavefunctions of the normal gas are given by eigenequations which are similar to the Bogoliubov equations. The excitation spectra and the wavefunctions constitute the density of the normal gas.

Within the Bogoliubov ($T = 0$) approximation, the occurrence and the disappearance of a vortex are indicated by the existence of an excitation with negative excitation energy (in other words, the anomalous excitation). There also exist relations between the direction of the precessional motion of the vortex and the sign of the excitation energies within zero-temperature theories. This paper aims to answer the following question: Does this relation stay valid in the Popov ($T > 0$) approximation?

Besides the problem of the direction of precession, the precession frequency within the Popov approximation has not been investigated in detail. The precession fre-

quency at zero temperature has been discussed within the Thomas-Fermi (TF) approximation using several methods (see Sec. 5.1 of Ref. [8] and Ref. [9]). There also exists an analysis within the classical-field approximation [10] in finite-temperature systems.

The condensate is assumed to be trapped with a rotationally symmetric trap. Therefore, a precessing vortex is an off-centered vortex. Within zero-temperature theories, a static system with an off-centered vortex [11] in the rotating frame is equivalent to a system in the presence of a precessing vortex. If the displacement Δr of the vortex from the trap center is small, the excitation energy of the anomalous mode [12], or the core-localized mode depends linearly on the rotation frequency. The variational Lagrangian analysis used in Ref. [12] and Bogoliubov theory yield the same dependence for a centered vortex.

In a previous study [13], we discussed a precessing vortex state as a deviation from the axisymmetric configuration. In this work we aim to treat the precessing vortex in a 2D geometry directly within the Popov approximation in order that the relation between the precession and the excitations are directly taken into account from the outset.

II. APPROXIMATIONS

The condensate is treated with a nonlinear Schrödinger equation (NLSE) within the Popov approximation. The thermal atoms are described using the Popov equations which are eigenequations. Because of computational complexity, we use the Popov equations only for excitations below a certain cutoff energy E_{cut} . The excitation energies $\varepsilon > E_{\text{cut}}$ are taken into account within the semiclassical approximation [14, 15, 16]. The density of the condensate is $n_0(\mathbf{r}) \equiv |\phi(\mathbf{r})|^2$, where $\phi(\mathbf{r})$ is the condensate wavefunction. The normal particle density coming from the excitations below (above) E_{cut} is n_1 (n_2). Therefore, the particle number density is $n(\mathbf{r}) = n_0(\mathbf{r}) + n_1(\mathbf{r}) + n_2(\mathbf{r})$. The condensate is described with the NLSE

$$\{-C\nabla^2 + V - \mu + g(n_0 + 2n_1 + 2n_2) - \boldsymbol{\omega}_{\text{rot}} \cdot \mathbf{r} \times \mathbf{p}\} \phi = 0 \quad (1)$$

*Electronic address: tomoya@focus.hut.fi

where $C = \hbar^2/(2m)$ and $g = 4\pi\hbar^2a/m$. The mass of a Na atom $m = 38.17 \times 10^{-27}$ kg, and the scattering length $a = 2.75$ nm for Na atoms are employed. We use the cutoff energy $E_{\text{cut}} = 10\hbar\omega_{\text{tr}}$ [17]. Angular velocity of rotation is ω_{rot} and the rotation axis is parallel with the z axis ($\omega_{\text{rot}} = e_z\omega_{\text{rot}}$). Excitations below the cutoff E_{cut} are eigenstates of the Popov equations

$$\{-C\nabla^2 + V - \mu + 2g(n_0 + n_1 + n_2) - \omega_{\text{rot}} \cdot \mathbf{r} \times \mathbf{p}\}u_q - g\phi^2v_q = \varepsilon_q u_q, \quad (2a)$$

$$-\{-C\nabla^2 + V - \mu + 2g(n_0 + n_1 + n_2) + \omega_{\text{rot}} \cdot \mathbf{r} \times \mathbf{p}\}v_q + g\phi^{*2}u_q = \varepsilon_q v_q. \quad (2b)$$

These reduce to the Bogoliubov equations if we neglect n_1 and n_2 . The wavefunctions u_q and v_q obey the normalization condition

$$\int (|u_q|^2 - |v_q|^2) d\mathbf{r} = 1. \quad (3)$$

The density n_1 is a weighted sum of the wavefunctions u and v :

$$n_1(\mathbf{r}) = \left\{ \sum_{q(\varepsilon_q < E_{\text{cut}})} (|u_q|^2 + |v_q|^2) f(\varepsilon_q) + |v_q|^2 \right\} \quad (4)$$

$$f(\varepsilon) = \frac{1}{e^{\varepsilon/(k_B T)} - 1}. \quad (5)$$

The higher-energy range $\varepsilon > E_{\text{cut}}$ is described within the semiclassical approximation [14, 15, 16] which neglects the derivatives of the amplitudes of the wavefunctions u and v and the second derivatives of their phases. We also neglect the phase of the condensate wavefunction ϕ here. Then the Popov equations (2) reduce into algebraic form (Ref. [16], Eqs. (5)). The expression for n_2 , in analogy with Eq. (4), is:

$$n_2(\mathbf{r}) = \int \frac{d\mathbf{p}}{\hbar^3} \left\{ \frac{\varepsilon_{\text{HF}}}{\tilde{\varepsilon}} \left(f(\varepsilon) + \frac{1}{2} \right) - \frac{1}{2} \right\} \Theta(\varepsilon - E_{\text{cut}}) \quad (6)$$

where the Hartree-Fock (HF) energy

$$\varepsilon_{\text{HF}}(\mathbf{r}, \mathbf{p}) = \frac{\mathbf{p}^2}{2m} + V - \mu + 2g(n_0 + n_1 + n_2) \quad (7)$$

and energies

$$\tilde{\varepsilon}(\mathbf{r}, \mathbf{p}) = \sqrt{\varepsilon_{\text{HF}}^2(\mathbf{r}, \mathbf{p}) - g^2n_0}, \quad (8)$$

$$\varepsilon(\mathbf{r}, \mathbf{p}) = \tilde{\varepsilon}(\mathbf{r}, \mathbf{p}) - \omega_{\text{rot}} \cdot \mathbf{r} \times \mathbf{p} \quad (9)$$

are functions of \mathbf{r} and \mathbf{p} . The noncondensate densities n_1 and n_2 are determined from Eqs. (4) and (6). They are treated as mean field potentials throughout the above equations. Thus the numerical procedure needs to be selfconsistent such that it is repeated until the solution reaches convergence in which all the equations are simultaneously satisfied.

The angular momenta of the condensate ϕ and of the wavefunctions u, v are

$$\mathcal{A}(\phi) = \mathbf{e}_z \cdot \frac{\int \phi^*(\mathbf{r} \times \mathbf{p})\phi d\mathbf{r}}{\hbar \int n_0(\mathbf{r}) d\mathbf{r}}, \quad (10)$$

$$\mathcal{A}(u_q) = \mathbf{e}_z \cdot \frac{\int u_q^*(\mathbf{r} \times \mathbf{p})u_q d\mathbf{r}}{\hbar U_q}, \quad (11)$$

$$\mathcal{A}(v_q) = \mathbf{e}_z \cdot \frac{\int v_q^*(\mathbf{r} \times \mathbf{p})v_q d\mathbf{r}}{\hbar V_q} \quad (12)$$

where $U_q \equiv \int |u_q|^2 d\mathbf{r}$ and $V_q \equiv \int |v_q|^2 d\mathbf{r}$. Within the Bogoliubov theory ($T = 0$), the excitation energies depend linearly on the angular velocity ω_{rot} as follows:

$$\varepsilon = \varepsilon_{\text{lab}} - \hbar\omega_{\text{rot}}q_\theta, \quad (13)$$

$$q_\theta \equiv \text{Re}[\{\mathcal{A}(u_q) - \mathcal{A}(\phi)\}U_q + \{\mathcal{A}(v_q) + \mathcal{A}(\phi)\}V_q] / (U_q + V_q). \quad (14)$$

The value q_θ is useful for characterizing [2, 3] an excitation also for finite-temperature systems. But as for the ω dependence of ε , there are deviations from Eq. (13) due to changes of density in the normal component $n_1(\mathbf{r}) + n_2(\mathbf{r})$ for finite-temperature systems. Figure 1 indicates these deviations. Changes in the excitation energies modify the normal-component density which in turn affects the whole system, including the ε 's themselves. Therefore, the spectra for each value of ω_{rot} needs to be calculated individually.

III. OFF-CENTERED VORTEX

The sign of the excitation energy of the core-localized excitation and the direction of the precessional motion are related [12] at zero temperature. The predicted precession frequency fits well with results of the experiments [18]. A finite-temperature extension of the Bogoliubov equation, the Popov approximation, shows that the sign of the core-localized excitation becomes positive [19, 20]. If the direction of the precessing motion and the sign of the excitation energy correspond to each other, the precessing motion of the vortex must also be inverted as the lowest excitation energy raises from negative to positive values.

We extend the 2D treatment [11] of the Bogoliubov equations to finite-temperature Popov equations. It makes possible to treat the slightly off-centered vortices directly within the Popov approximation.

Assume a BEC system has a vortex line perpendicular to the z axis. Particles are confined with a harmonic trap along the x and y axes

$$V(x, y) = \frac{m\omega_{\text{tr}}^2}{2}(x^2 + y^2) \quad (15)$$

with $\omega_{\text{tr}} = 2\pi \times 200$ Hz. The system has finite z thickness and it is uniform along the z axis. Periodic boundary conditions along z are used. Hence this system is

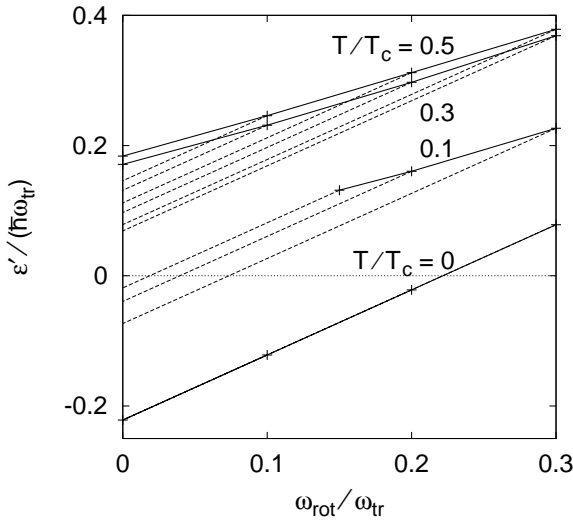


FIG. 1: Dependence of ε' (lowest ε) on ω_{rot} in an axisymmetric system ($\Delta r = 0$). The solid lines indicate the ε' at $T = 0$ (Bogoliubov approximation) and $T/T_c = 0.1, 0.3$, and 0.5 (Popov approximation). The dotted lines represent Eq. (13). The angular momentum $q_\theta = -1$. The dotted line and the solid line overlap at $T = 0$. The two lines are separated for $T > 0$, which means that “equality” between the rotation velocity ω_{rot} and the excitation energy in Eq. (13) is lost at finite temperatures.

not a two-dimensional BEC [21, 22], but rather a three-dimensional BEC having restricted geometry. We treat a system having 10^5 atoms within a z thickness of $10 \mu\text{m}$. The Thomas-Fermi (TF) radius $R_{\text{TF}} = 6.793 \mu\text{m}$ is used as the scale of length.

Equations (1) - (9) are repeatedly solved until convergence into a self-consistent solution. While the vortex-free ($\mathcal{A}(\phi) = 0$) and centered-vortex ($\mathcal{A}(\phi) = 1$) configurations are most likely, there also exists a solution with an off-centered vortex ($0 < \mathcal{A}(\phi) < 1$) in a narrow window of ω . Figures 2(a-c) represent such a typical system. Here the angular momentum is $\mathcal{A}(\phi) = 0.863$. The particle number of the condensate is 48% of the total particle number. The noncondensate density has a characteristic peak at the core of the vortex, like those in the axisymmetric studies [19, 20].

The displacement of the vortex core Δr is unrestricted in the numerical processes, unlike for the axisymmetric situations ($\Delta r = 0$). Therefore, the displacement Δr depends on temperature T and the rotation frequency ω_{rot} as presented in Fig. 3(a).

Figure 3(a) plots rotation frequencies at which the system is static. Let us denote the displacement and the rotation frequency at the static point as $\Delta r'$ and ω'_{rot} . When $\Delta r < \Delta r'$, $\omega_{\text{rot}} = \omega'_{\text{rot}}$, and $T = 0$, the vortex has an instability and it tends to move inward. When $\Delta r > \Delta r'$, the direction is outward. As ω_{rot} increases in Fig. 3(a), the system has a wider range of displacements

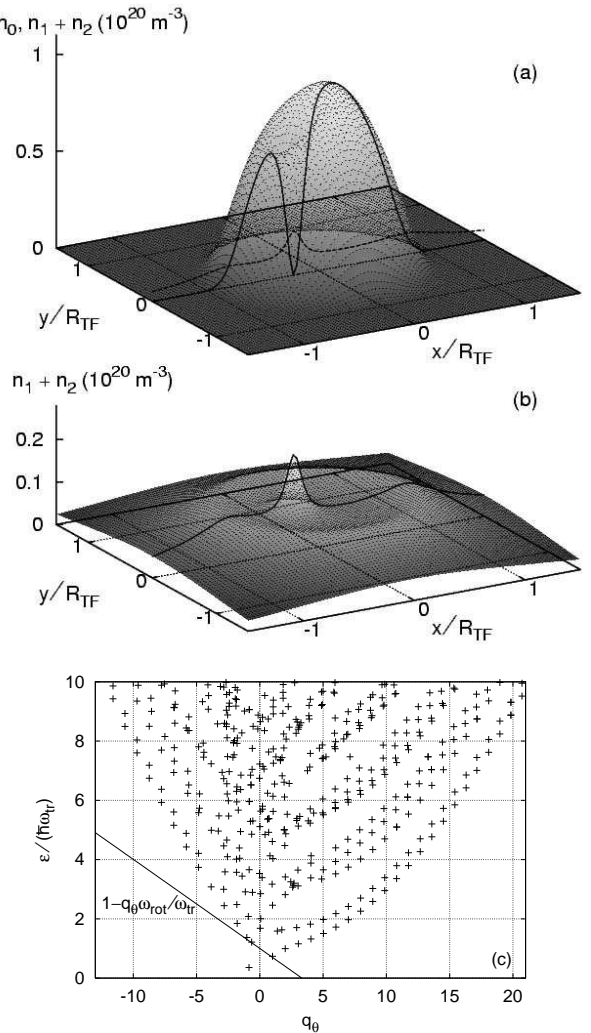


FIG. 2: Density profiles of a system at the temperature $T = 0.5 T_c$, and angular momentum of the condensate $\mathcal{A}(\phi) = 0.863$ in rotating coordinates with $\omega_{\text{rot}} = 0.300 \omega_{\text{tr}}$. (a) Particle density $n_0(x, y)$ of the condensate, (b) Particle density $n_1(x, y) + n_2(x, y)$ of the noncondensate, (c) Excitation spectra ε_q vs. q_θ . The solid line shows $1 - \omega_{\text{rot}} q_\theta / \omega_{\text{tr}}$. Its slope indicates the rotation velocity ω_{rot} . The line touches the dipole modes at $q_\theta = \pm 1$.

Δr having an inward instability. This instability brings the vortex to the center of system and makes the vortex state more sustainable.

The lowest excitation energies ε' in Fig. 3(b) differ significantly between the $T = 0$ system and those of the $T = 0.1 T_c$ system. It is small and negative ($0 > \varepsilon' > -0.004 \hbar \omega_{\text{tr}}$) for the $T = 0$ system, while it is positive in the $T = 0.1 T_c$ system. The corresponding rotation frequencies ω_{rot} in Fig. 3(a) differ only a little. This indicates that the direction of the precessional motion which is represented by the sign of ω_{rot} and the sign of the lowest core excitation energy are not related in the $T > 0$ systems. This point is discussed further in the

next section.

Figures 4(a-b) compare the spectral densities

$$g_1(j) = \int d\mathbf{r} \sum_{q,j \leq \frac{\varepsilon_q}{\hbar\omega_{\text{tr}}} < (j+1)} (|u_q|^2 + |v_q|^2) f(\varepsilon_q) + |v_q|^2, \quad (16)$$

$$g_2(\varepsilon'') = \int \frac{d\mathbf{p} d\mathbf{r}}{\hbar^3} \left\{ \frac{\varepsilon_{\text{HF}}}{\tilde{\varepsilon}} \left(f(\varepsilon) + \frac{1}{2} \right) - \frac{1}{2} \right\} \delta(\varepsilon'' - \varepsilon) \quad (17)$$

and the angular momenta of the noncondensate

$$L_1(j) = \mathbf{e}_z \cdot \frac{1}{\hbar} \sum_{q,j \leq \frac{\varepsilon_q}{\hbar\omega_{\text{tr}}} < (j+1)} \int d\mathbf{r} [\{u_q^*(\mathbf{r} \times \mathbf{p}) u_q + v_q(\mathbf{r} \times \mathbf{p}) v_q^*\} f(\varepsilon_q) + v_q(\mathbf{r} \times \mathbf{p}) v_q^*], \quad (18)$$

$$L_2(\varepsilon'') = \mathbf{e}_z \cdot \frac{1}{\hbar} \int \frac{d\mathbf{p} d\mathbf{r}}{\hbar^3} (\mathbf{r} \times \mathbf{p}) \{f(\varepsilon(\mathbf{r}, \mathbf{p})) - \frac{1}{2} \left(\frac{\varepsilon_{\text{HF}}(\mathbf{r}, \mathbf{p})}{\tilde{\varepsilon}(\mathbf{r}, \mathbf{p})} - 1 \right)\} \times \delta(\varepsilon'' - \varepsilon) \quad (19)$$

to verify the mutual consistency of the Popov approximation and that of the semiclassical approximation. Above, g_1 and L_1 are obtained within the Popov approximation, while g_2 and L_2 are obtained within the semiclassical approximation. Results of these two approximations are consistent with each other for $\varepsilon > 5 \hbar\omega_{\text{tr}}$.

The core-localized mode is mainly affected by the particle densities inside the core, while g_1 and g_2 account for the densities over the whole area of the system. Since our main interest is the core-localized mode, we employ calculations with reduced accuracy for n_2 and g_2 for larger x, y (around $|x| > 1.2R_{\text{TF}}$ or $|y| > 1.2R_{\text{TF}}$). This affects the plot for g_i in Fig. 4(a), but it has little effect on ε' as shown in the dependence [17] of ε' on the cutoff energy, E_{cut} .

IV. THE SIGN AND DIRECTION OF VORTEX PRECESSION

The angular velocity ω_{prec} of the precessional motion of a vortex is related with that of the rotating frame ω_{rot} through

$$\omega_{\text{prec}} + \omega_{\text{rot}} = \text{const.} \quad (20)$$

within the GP equations. The core-localized excitation has the lowest excitation energy ε' within the range of ω_{rot} we treat. Using variational Lagrangean analysis [12], it can be shown that

$$\varepsilon' = 0 \text{ at } \omega_{\text{prec}} = 0 \quad (21)$$

for a small displacement Δr . This relation remains valid for $0 < \Delta r < 0.5R_{\text{TF}}$ within the accuracy $0 > \varepsilon' > -0.004\hbar\omega_{\text{tr}}$ in the present system, see Fig. 3(b).

Equations (13), (20), and (21) lead to the relation

$$\varepsilon' = \hbar q \omega_{\text{prec}}. \quad (22)$$

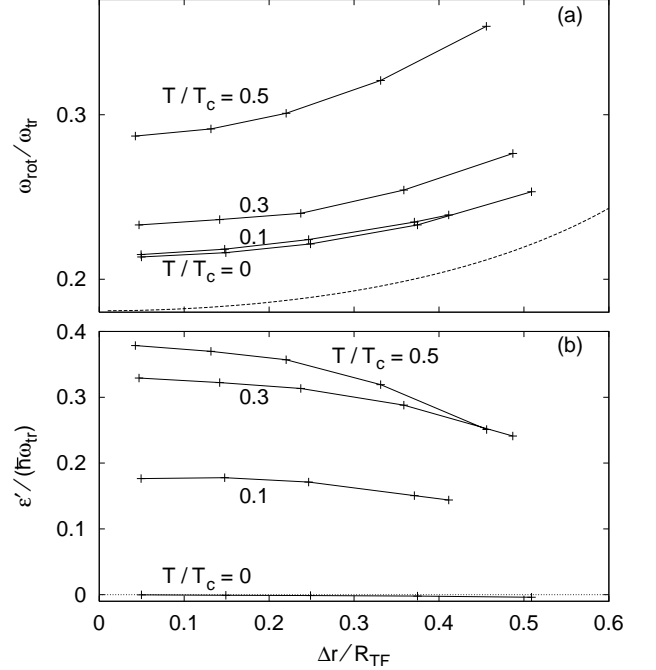


FIG. 3: Horizontal axis indicates the displacement Δr of the vortex core from the center of the harmonic trap. (a) The vertical axis is the angular velocity ω_{rot} of the rotating coordinates for temperatures $T = 0.0, 0.1, 0.3$, and $0.5 T_c$. The difference in the frequencies is less than 2% between a point at $T = 0$ and a corresponding one at $T = 0.1 T_c$ within $\Delta r < 0.4$. The dotted line is the result of the TF approximation at $T = 0$ [9]. Our results for $T = 0.1 T_c$ are 16–19% above those of the TF approximation. (b) The lowest excitation energy. All of the energies in the finite-temperature ($T = 0.1, 0.3$ and 0.5) systems are positive. The energy of the lowest core localized excitation only turns negative for $T = 0$ when the normal densities n_1 and n_2 are neglected.

Therefore, the direction of the precessional motion and the sign of the core-localized excitation correspond to each other at $T = 0$.

If the coordinate transformation in Eq. (20) were not valid, the relation Eq. (22) between the excitation energy ε' and the angular velocity ω_{prec} of the precessional motion would not hold. The next section describes how this occurs at finite temperatures.

An easier way to disprove Eq. (22) is as follows. Figure 3 (b) displays ε' for $\omega_{\text{prec}} = 0$. It shows that Eq. (21) is no longer satisfied for $T > 0$. Therefore, it becomes impossible to satisfy Eq. (22). The sign of the lowest excitation and the direction of the precessional motion are no longer related within the finite-temperature (Popov) approximation.

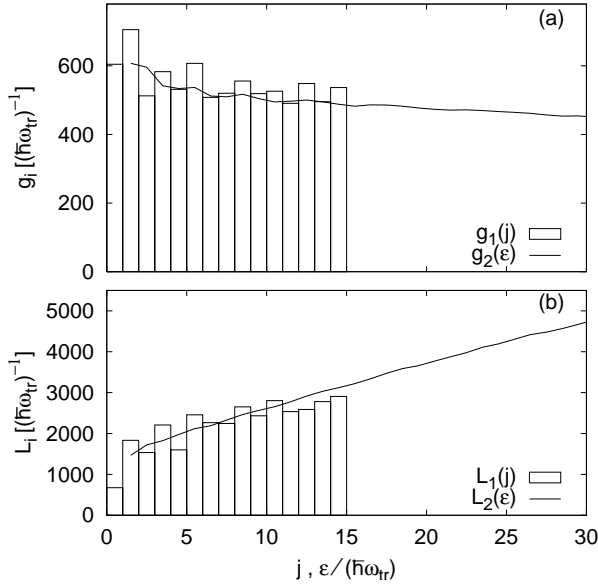


FIG. 4: (a) Spectral distributions $g_1(\epsilon)$ obtained within the Popov approximation and $g_2(\epsilon)$ obtained within the semiclassical approximation. (b) Angular-momentum distributions L_1 and L_2 . These two approximations yield consistent particle numbers and angular momenta for a wide range of energies. The temperature $T/T_c = 0.5$ and the angular momentum $\mathcal{A}(\phi) = 0.863$.

V. PRECESSING AND ROTATING FRAMES

We have presented density profiles of an off-centered vortex within the rotating frame. This frame mimics a system of atoms in a rotating trap although the deformation of the trapping potential is not included explicitly. The vortices are precessing if we observe them from the nonrotating frame. But there is a restriction in the velocity of the precession.

Let us compare the velocities of the noncondensate and the angular velocity of the frame ω_{rot} at $\omega_{\text{prec}} = 0$. Figure 5 (a) displays the local velocities on the x axis for the system. The velocities

$$\mathbf{V}_{12}(\mathbf{r}) = \frac{\text{Re}[\mathbf{P}_1(\mathbf{r}) + \mathbf{P}_2(\mathbf{r})]}{m \{n_1(\mathbf{r}) + n_2(\mathbf{r})\}}, \quad (23)$$

$$\mathbf{V}(\mathbf{r}) = \frac{\text{Re}[\mathbf{P}_0(\mathbf{r}) + \mathbf{P}_1(\mathbf{r}) + \mathbf{P}_2(\mathbf{r})]}{mn(\mathbf{r})} \quad (24)$$

which are particle-current densities divided by the particle densities; they are defined using the momentum den-

sities

$$\mathbf{P}_0(\mathbf{r}) = \phi^*(\mathbf{r}) \mathbf{p} \phi(\mathbf{r}), \quad (25)$$

$$\mathbf{P}_1(\mathbf{r}) = \sum_{q (\epsilon_q < E_{\text{cut}})} \{u_q^*(\mathbf{r}) \mathbf{p} u_q(\mathbf{r}) + v_q(\mathbf{r}) \mathbf{p} v_q^*(\mathbf{r})\} f(\epsilon_q) + v_q(\mathbf{r}) \mathbf{p} v_q^*(\mathbf{r}), \quad (26)$$

$$\mathbf{P}_2(\mathbf{r}) = \int \frac{d\mathbf{p}}{\hbar^3} \mathbf{p} \left\{ f(\epsilon(\mathbf{r}, \mathbf{p})) - \frac{1}{2} \left(\frac{\epsilon_{\text{HF}}(\mathbf{r}, \mathbf{p})}{\tilde{\epsilon}(\mathbf{r}, \mathbf{p})} - 1 \right) \right\} \times \Theta [\epsilon(\mathbf{r}, \mathbf{p}) - E_{\text{cut}}]. \quad (27)$$

The velocity closely follows that of the rotating frame outside of the condensate ($|x| > R_{\text{TF}}$) in Fig. 5(a). It is straightforward to show that $\mathbf{V}(\mathbf{r})$ reduces to

$$\mathbf{V}(\mathbf{r}) = \omega_{\text{rot}} (-y, x, 0) \quad (28)$$

for large $|\mathbf{r}|$ where the density of the condensate and normal component below the cutoff are negligible ($n_0 + n_1 \ll n$). This indicates adiabaticity between the rotating trap and the normal gas. Within the Popov approximation, the angular velocity of the precessional motion of a vortex is restricted to that of a normal gas and a confining trap.

We have considered static systems with $\omega_{\text{prec}} = 0$ in a rotating frame with the angular velocity ω_{rot} . These two ω 's may be transformed between each other using the simple relationship between the stationary and rotating frames of reference in Eq. (20), valid at zero temperature. But taking into account the normal component, this relation is only valid when the normal component is rotating at the angular velocity ω_{rot} . Varying ω_{rot} will change the density profiles through Eqs. (9) and (13). Then the coordinate transformation Eq. (20) does not hold. Adiabaticity required within the Popov framework restricts the recognizing of ω_{rot} as the angular velocity of precession ω_{prec} . This is another reason why Eq. (22) does not hold at finite temperatures.

VI. DISCUSSION

It is confirmed that the sign of the lowest excitation energy ϵ' is, in general, unrelated with the direction of the precessional motion of a vortex within the Popov approximation. Within the Bogoliubov approximation, the excitation energy ϵ' of core-localized mode and the precession frequency ω_{prec} are proportional to each other as shown in Eq. (22). The derivation of Eq. (22) shows that the angular velocity (and the direction) ω_{prec} of the precessional motion arises from the coordinate transformation Eq. (20), which does not have any explicit relation with the core-localized excitation. Therefore, the core-localized excitation is responsible for the inward/outward motions of vortex and not explicitly related to the precessional motion.

We think that this nature of the core-localized excitation does not change even at a finite T . However, a

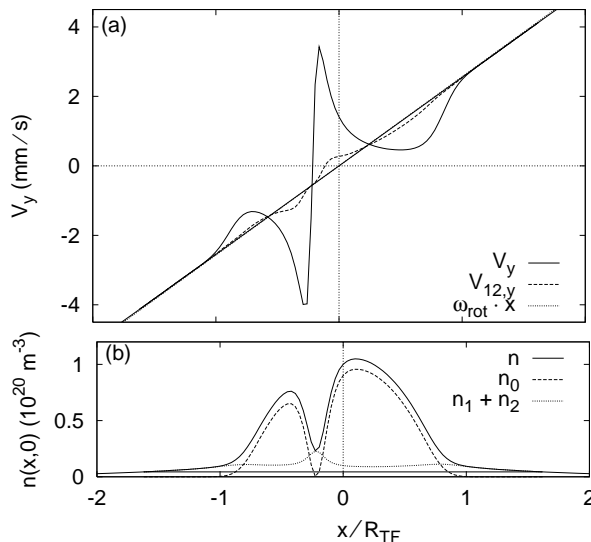


FIG. 5: (a) Velocities of all the atoms (solid line) and the normal component (dashed line) along the x axis ($y = 0$). The velocity follows that of the rotating frame (dotted line) outside the condensate ($|x| > R_{TF}$). Temperature $T = 0.5T_c$ and angular momentum $A(\phi) = 0.863$. (b) Density profiles along the x axis for comparison with (a). The plots of n_0 (dashed line) and $n_1 + n_2$ (dotted line) are equivalent to those on the x axes in Figs. 2(a-b).

system described within the Popov approximation cannot undergo the coordinate transformation. Within the

Popov approximation, the velocity ω_{rot} in Fig. 3(a) may be recognized as the angular velocity of the precessional motion only when the condition of adiabaticity is obeyed. Therefore, the relation between the sign of the lowest excitation energy ϵ' and the sign of ω_{prec} , *i.e.*, the direction of the precessional motion of a vortex is broken within the Popov approximation.

We obtained the precession frequencies of a vortex at finite temperatures. The vortex-precession frequency manifests [Fig. 3(a)] the same tendency as a function of displacement Δr as the zero-temperature TF studies [8, 9]. The precession frequency increases as the displacement Δr and the temperature increase. The frequencies differ only little between those for $T = 0$ and $T = 0.1T_c$, despite the large changes in the excitation spectra. Although a pinning effect [19, 20, 21] caused by the normal component makes a significant difference in the excitation energy ϵ' , it has little effect on the precession frequencies between the systems at zero and finite temperatures.

Acknowledgements

The authors are grateful to G. Baym, E. Lundh, M. Möttönen, and S. M. M. Virtanen for stimulating discussions. One of the authors (T.I.) is supported by the bilateral exchange program between the Academy of Finland and JSPS, the Japan Society for the Promotion of Science.

[1] C. J. Pethick and H. Smith, *Bose-Einstein Condensation in Dilute Gases* (Cambridge University Press, Cambridge, England, 2002).

[2] L. O. Baksmaty, S. J. Woo, S. Choi, and N. P. Bigelow, e-print cond-mat/0307368; S. J. Woo, L. O. Baksmaty, S. Choi, and N. P. Bigelow, e-print cond-mat/0308431.

[3] T. Mizushima, Y. Kawaguchi, K. Machida, T. Ohmi, T. Isoshima, and M. M. Salomaa, e-print cond-mat/0308010.

[4] C. Tozzo and F. Dalfovo, New J. Phys. **5**, 54 (2003).

[5] M. J. Davis, S. A. Morgan, and K. Burnett, Phys. Rev. Lett. **87**, 160402 (2001).

[6] E. Zaremba, A. Griffin and T. Nikuni, Phys. Rev. A **57**, 4695 (1998); T. Nikuni, Phys. Rev. A **65**, 033611 (2002).

[7] F. Dalfovo, S. Giorgini, L. P. Pitaevskii and S. Stringari, Rev. Mod. Phys. **71**, 463 (1999).

[8] A. L. Fetter and A. A. Svidzinsky, J. Phys.:Condens. Matter **13**, R135 (2001).

[9] E. Lundh and P. Ao, Phys. Rev. A **61**, 063612 (2000).

[10] H. Schmidt, K. Góral, F. Floegel, M. Gajda, and K. Rzażewski, J. Opt. B **5**, S96 (2003).

[11] T. Isoshima, J. Huhtamäki, and M. M. Salomaa, Phys. Rev. A **68**, 033611 (2003).

[12] M. Linn and A. L. Fetter, Phys. Rev. A **61**, 063603 (2000).

[13] S. M. M. Virtanen, T. P. Simula, and M. M. Salomaa, Phys. Rev. Lett. **87**, 230403 (2001).

[14] S. Giorgini, L. P. Pitaevskii, and S. Stringari, Phys. Rev. A **54**, R4633 (1996).

[15] F. Dalfovo, S. Giorgini, M. Guilleumas, L. Pitaevskii, and S. Stringari, Phys. Rev. A **56**, 3840 (1997).

[16] J. Reidl, A. Csordás, R. Graham, and P. Szépfalusy, Phys. Rev. A **59**, 3816 (1999).

[17] The choice for the cutoff has very little effect on the energy ϵ' of the core-localized mode. At $T/T_c = 0.5$ and $A(\phi) = 0.863$, the energies ϵ' for various cutoff values are $(E_{\text{cut}}/(\hbar\omega_{\text{tr}}), \epsilon'/(\hbar\omega_{\text{tr}})) = (5, 0.345), (10, 0.354)$, and $(20, 0.357)$.

[18] D. L. Feder, A. A. Svidzinsky, A. L. Fetter, and C. W. Clark, Phys. Rev. Lett. **86**, 564 (2001).

[19] T. Isoshima and K. Machida, Phys. Rev. A **59**, 2203 (1999).

[20] S. M. M. Virtanen, T. P. Simula, and M. M. Salomaa, Phys. Rev. Lett. **86**, 2704 (2001).

[21] L. Pricoupenko, e-print cond-mat/0309212.

[22] C. Gies, B. P. van Zyl, S. A. Morgan, and D. A. W. Hutchinson, e-print cond-mat/0308177.